Geochemistry and K-Ar Age of the Imog Granite at the southwestern Part of the Hambaeg Basin, Korea*

Young Kook Hong**

Abstract: The Cretaceous Imog granite is a calc-alkaline, subsolvus monzogranite and shows characteristics of "I-type" and "magnetite-series" granite by mineralogy and chemical composition. Many of the major and trace element characteristic of the Imog granite are consistent with a relationship by fractional crystallization of a basic magma. The primary magma of the granite derived from the subduction of oceanic crust at the destructive plate margin. The granite shows light REE enrichment with $(Ce/Yb)N$ ratios of $7.77 \sim 12.55$. All the REE patterns show Eu negative anomalies $(Eu/Eu^* = 0.69)$ in the pluton.

The Imog granite at the southwestern part of the Hambaeg basin may be intruded along the tectonic intersections of the E-W and N-S lines such as deep faults and fractures. Radiometric age determination on the granite reveals as $96.7 \pm 2.0 Ma$ by K-Ar dating on biotite.

INTRODUCTION

There are many contact metasomatic ore deposits around the Hambaeg basin in the northeastern part of South Korea (Fig. 1a); Sangdong (W-Mo), Geodo (Cu-Fe-Ag), Wondong (W-Mo-Pb-Zn-Fe-Cu), Dongnam (Fe-Mn-Au-As-Mo-Pb-Zn), Shinyemi (Fe-Mo-Pb-Zn) and Imog (Pb-Zn) mines.

The Hambaeg basin where the Pyeongan Group dominates, is composed of the Carboniferous to Triassic non-marine sedimentary rocks. The Pyeongan Group mainly consisted of sandstone and shale, and one of the main productive coal-bearing formations in Korean Peninsula. The host rocks of the mineral deposits are the Cambro-Ordovician Joseon Supergroup in which the limestones are predominant. The ore doposits around the Hambaeg basin are closely associated with the Cretaceous plutonism and Joseon Supergroup, that is quite different from the Cretaceous

granites intruding the Gyeongsang sedimentary basin in which volcanic and non-marine sedimentary rocks are abundant. The studied Imog granite cropping out about $6km^2$ ($3km \times 2km$) is located in the southwestern limb of the Hambaeg basin (Fig. 1a). The purpose of this work is to provide petrogenesis of the granite. In this paper, a new K-Ar age determination on biotite is also reported.

GEOLOGIC SETTING

The general geology of the Imog granite was mapped at 1:50,000 scale by Lee (1966). The petrochemical works were previously carried out by Kim and Kim (1978), Yun (1985), and Kim (1986).

The geology of the studied area comprises Precambrian Yulri Group, Cambro-Ordovician Joseon Supergroup and Imog granite (Fig. 1b). The Precambrian Yulri Group is composed of biotite-sericite schist, micaceous quartz schist and argillaceous sandy quartzite. The Cambro-Ordovician Joseon Supergroup consists of Cambrian Jangsan light brown to buff quartzite,
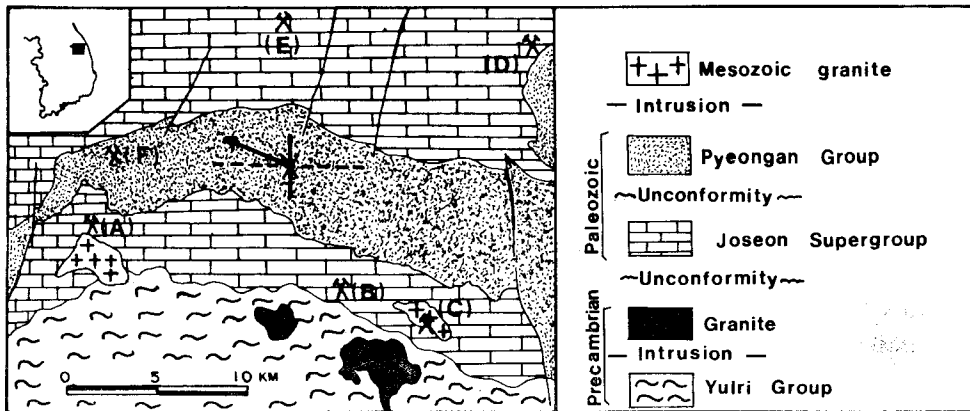
Fig. 1a Regional geology of the Hambaeg basin. The metallic ore deposits are as follows; A(Imog), B(Sangdong), C(Geodo), D(Wondong), E(Dongnam) and F(Shinyemi).
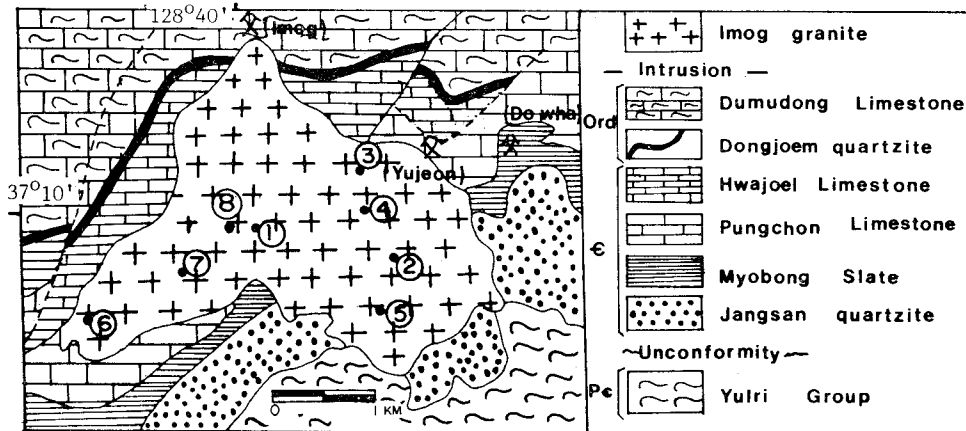

Fig. 1b Geological map and sample locations of the Imog granite (after Lee 1966).
①~⑧; Sample locations

Myobong slate, Ordovician Pungchon limestone, Hwajeol impure limeston, Dongjeom quartzite and Dumudong impure limestone. The Imog granite intruding the Yulri Group and Joseon Supergroup is generally medium grained pale pinkish feldspar biotite granite and showing porphyritic texture with phenocrysts of pinkish alkali-feldspar. The granite is largely homogeneous in texture and mineral composition over the whole area. Small and rounded mafic carbonaceous xenoliths are observed in many places, especially around the marginal part of the pluton. In particular, the subangular to rounded biotite-rich xenoliths are abundant at the southern part

of the granite where sample IM.1 was collected (Fig. 1b). The size of xenolith varies from 8cm×5cm to 15cm×10cm. The biotite-rich xenolith may be the result of the dissolution of the Myobong slate in the granitic magma. Aplitic dykes are also found in the granite. The granite is emplaced at the shallow level with sharp contact, gives the country rocks thermal metamorphism and in part skarnization within limestone. The detailed regional minaralization was investigated by Seo (1985). The Imog, Yujeon and Dowhadong mines are located in the NE part of the granite contact zone (Fig. 1b). The type of ore deposits are contact metasomatic and

fissure filling. Ore minerals are mainly galena and sphalerite with small amount of pyrite, chalcopyrite, arsenopyrite and pyrrhotite.

PETROGRAPHY

The Imog granite consists of quartz (31% modal); microcline-microperthite (22%); oligoclase (35%); biotite (8%); hornblende (1.5%); apatite, zircon, tourmaline and opaques (2.5%). Quartz crystals occur generally subhedral to anhedral grains with suture texture. The medium to coarse grained quartz shows undulatory extinctions with an average of 2~3 mm across. Some quartz in the form of aggregates are interlocked with each other, which are probably due to shear stress. Alkali feldspar occurs almost exclusively as microperthite. String type of the microcline and microperthite is predominant and overgrown by zoned plagioclase. Plagioclase ranges in composition from An_{18} to An_{26} as oligoclase. Albite-twinning is dominant, but zoned structures are also observed. Zoning in the plagioclase may be caused by either hypabyssal intrusion or fluctuations of physicochemical conditions at the time of crystallization. Biotite as flakes shows poikilitic texture with inclusions of apatite, zircon and opaques. Some of dark brown biotite crystals are overgrown on hornblendes. Tourmaline is one of the last minerals to crystallize and cuts previously formed minerals. The modal compositions of the samples are plotted on a quartz-alkali feldspar-plagioclase diagram for classification (Streckeisen, 1976). The studied granite plots in the region of the monzogranite with a limited compositional variations.

MAGNETIC SUSCEPTIBILITY

The magnetic susceptibility in the Imog granite (Table 1) varies from 0.12 to 0.57$\times$ 10^{-3}cgs with an average of $(0.39\pm0.13)\times10^{-3}$ cgs unit equivalent to approximately 0.12% volume magnetite measured by SM-5 digital magnetic susceptibility meter (since 1×10^{-3}cgs$=$ 0.3% volume magnetite; Scintrex Instruction Manual, 1982). The magnetite content may be converted by $x=0.001V$ (Ishihara, 1979) where x is magnetic susceptibility in emu/g and V is volume percent of magnetite. Hence, the average 0.12% volume magnetite in the studied granite can be converted into 120×10^{-6}emu/g which belongs to "magnetite-series". Since the granitoids having the values higher than 100×10^{-6}emu/g are classified as "magnetite-series", while the lower ones as "ilmenite-series" (Ishihara and Ulriksen, 1980). The magnetite-series values seem to occur more widely than the ilmenite-series ones in the studied granite. The ilmenite-series values are seen in some places where carbonaceous xenoliths are abundant. They are resulted probably from local reduction due to admixing of the roof and wall sedimentary xenoliths.

GEOCHEMISTRY

The whole-rock geochemistry is based upon the analysis of 8 representative rocks. The localities of the analysed samples are shown in Fig. 1b. Major oxide elements were analysed by classical wet-method, trace elements were determined by X-ray fluorescence analysis on pressed powder pellets. Hf and Ta, and rare earth elements were obtained by instrumental neutron activation analysis (INAA) after the method of Gordon et al (1968). Details of sample preparation and analytical method are described by Hong (1983).

Major element abundances and norms for the granite are presented in Table 1. Important points of major element characteristics are outlined as follows: (1) The granite is classified chemically according to O'Connor (1965) using normative feldspar abundances. This classification is valid for rocks containing more than 10% of normative of modal quartz. In O'Connor's classification scheme, the Imog granite is plotted in

Table 1 Major element (wt. %) analyses and CIPW norms of the Imog granite (IM).
　　　　　M.S: Magnetic susceptibility in 10^{-3}cgs ($\times 10^{-6}$ emu/g).
　　　　　AV: Average, SD: standard deviation.

	IM. 1	IM. 2	IM. 3	IM. 4	IM. 5	IM. 6	IM. 7	IM. 8	AV.	SD.
SiO_2	66.14	66.76	67.50	67.16	67.70	67.86	67.96	67.54	67.33	0.62
TiO_2	0.20	0.23	0.23	0.15	0.18	0.22	0.20	0.17	0.20	0.03
Al_2O_3	16.73	16.78	16.01	15.79	16.59	16.08	15.42	15.66	16.13	0.51
Fe_2O_3	0.78	1.05	0.97	1.80	0.88	1.03	1.35	1.17	1.13	0.32
FeO	3.35	2.80	2.80	2.53	2.75	2.67	2.43	2.60	2.74	0.28
MgO	1.32	1.25	1.30	1.27	1.13	1.17	1.33	1.35	1.27	0.08
MnO	0.09	0.07	0.08	0.07	0.07	0.08	0.07	0.77	0.08	0.01
CaO	3.30	3.05	3.05	2.96	2.82	2.99	3.07	3.10	3.04	0.14
K_2O	4.16	4.01	3.95	4.19	4.00	4.01	4.01	3.82	4.02	0.12
Na_2O	3.34	3.34	3.30	3.31	3.42	3.30	3.38	3.47	3.36	0.06
P_2O_5	0.02	0.12	0.08	0.09	0.11	0.10	0.09	0.10	0.09	0.03
Ig. Loss	0.57	0.65	0.80	0.75	0.44	0.57	0.77	1.04	0.70	0.18
Total	100.00	100.11	100.07	100.07	100.09	100.08	100.08	100.09	100.07	0.03
Q	19.52	22.24	23.27	22.68	23.30	23.84	23.40	22.94	22.65	1.35
Or	24.73	23.83	23.52	24.93	23.72	23.81	23.86	22.79	23.90	0.67
Ab	28.43	28.42	28.13	28.20	29.04	28.06	28.80	29.65	28.59	0.54
An	16.33	14.43	14.72	14.20	13.33	14.26	14.75	14.87	14.61	0.85
Cr	0.79	1.69	0.96	0.64	1.77	1.12	0.15	0.42	0.94	0.57
Hy	8.60	7.11	7.33	6.18	6.93	6.72	6.44	7.02	7.04	0.73
Mt	1.14	1.53	1.42	2.63	1.28	1.50	1.97	1.71	1.65	0.47
Il	0.38	0.44	0.44	0.29	0.34	0.42	0.38	0.33	0.38	0.05
Ap	0.05	0.28	0.19	0.21	0.25	0.23	0.21	0.23	0.21	0.07
Fe_2O_3/FeO	0.23	0.38	0.35	0.71	0.32	0.39	0.56	0.45	0.42	0.15
K_2O/Na_2O	1.25	1.20	1.20	1.27	1.17	1.22	1.19	1.10	1.20	0.05
D. I.	72.68	74.49	74.92	75.81	76.06	75.71	76.06	75.38	75.14	1.14
M. S.	0.12	0.35	0.45	0.57	0.38	0.46	0.42	0.33	0.39	0.13
	(36)	(105)	(135)	(171)	(114)	(138)	(126)	(99)	(117)	(39)

the quartz monzonite region with a relatively narrow variation (Fig. 2) as suggested by modal compositions; (2) The K_2O/Na_2O ratios and D.I of the granite are invariable from 1.10 to 1.27
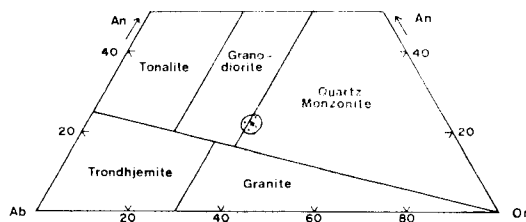
Fig. 2 Normative plots of Ab-Or-An showing field of the Imog granite (classification after O'Connor 1965).

with a mean of 1.20 and from 72.68 to 76.06 with an average of 75.14, respectively; (3) The variations in the abundance of major element show a little chemical change (Fig. 3) including AFM and NCK ternary diagrams because of eutectic crystallization; (4) Fe_2O_3/FeO ratios show low values ranging from 0.23 to 0.71 with an average of 0.42 ± 0.15 which may be resulted from the introduction of carbonaceous wall rocks (Joseon Supergroup) into the parental magma; (5) The alkalinity ratio (Wright, 1969) and calcium-oxide/alkalis against silica diagram (Brown, 1979) show that the Imog granite plots
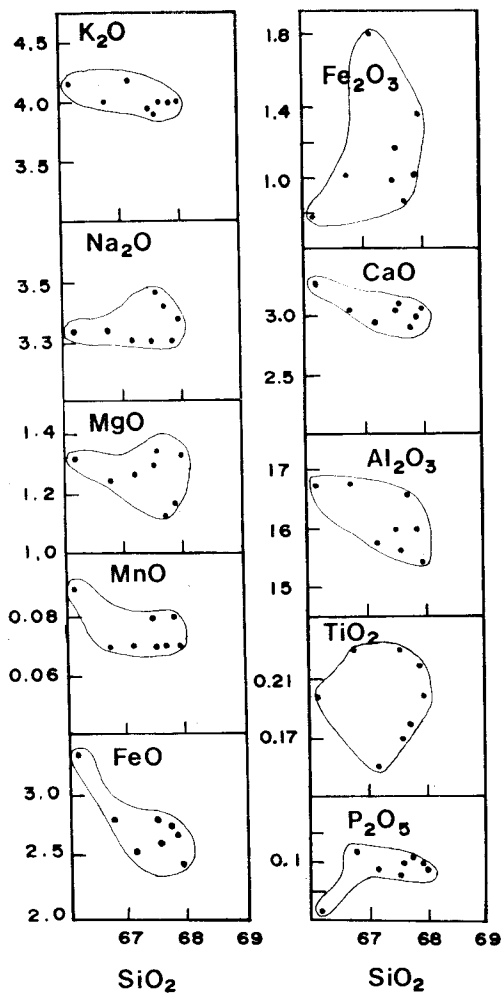
Fig. 3 Inter-element diagrams for major elements (Wt. %) in the Imog granite.

within the calc-alkaline field; (6) The normative corundum is relatively low which ranges from 0.42 to 1.77 with a mean of 0.94 and the molecular ratios of $Al_2O_3/(Na_2O+K_2O+CaO)$ ranging from 0.99 to 1.1 (1.05±0.04); (7) Normative proportion of Q-Ab-Or diagram illustrates a tight group with very little scatter, and lies near the thermal minima and low-pressure region with water saturated eutectic condition; (8) The ternary diagram of cations (Al-Na-K : Ca : Fe^{+2}+Mg) and variation diagram of (Fe_2O_3 : FeO) imply that the Imog granite is classified as "I-type" granite (Hine et

al., 1978).

The analytical results of trace element determinations are presented in Table 2. Rb contents in the granite range from 123ppm to 145ppm with a mean of 135ppm. Sr contents show a wide distribution ranging 85ppm to 160ppm (mean of 109±29ppm). Sr shows a positive correlation with Ba. The plot of Rb and Sr shows a negative relationship indicating that the variation could be dominated by plagioclase and alkai feldspar fractionation. The average Rb/Sr and K/Rb ratios illustrate 1.32 and 248, respectively. The positive and high correlation coefficients are found among the each group of elements such as La-Ba-Sr-Cr, Rb-Zr, Ce-Ag-Cu-U and Ni-Mo. Rb concentrations and Rb/Sr ratios show a progressive increase which is consistent with a crystallization. The Imog granite has enriched in LIL elements (K, Rb, Ba, Th, U, La, Ce) relative to HFS elements (Nb, Ta, Ti, Y). Low Ba and Sr contents imply that extensive crystallization of plagioclase in the magma (Fig. 4). Depletions of Nb, P and Y concentrations are mainly due to fractionation of apatite. High Zr content suggests that abundant magnetite and zircon concentration in the Imog granite.

The HFS elements, particularly Nb, Y, Ta, Yb and Zr are relatively immobile and are generally unaffected by postmagmatic alteration processes, which is why they have been used for discriminating tectonic settings in granitic rocks (Pearce et al 1984). Their behaviour is therefore regarded as a consequence of primary magmatic processes and must be examined in relation to fractionation. Granites may be subdivided according to their intrusive settings into four main groups such as ocean ridge granite, volcanic arc granite, within plate granite and collision granite (Pearce et al *op cit*). The Nb-Y, Ta-Tb and Rb-(Y+Nb) discriminant diagrams for the Imog granite show that the

Table 2 Trace element contents (in ppm) of samples from the Imog granite

	IM. 1	IM. 2	IM. 3	IM. 4	IM. 5	IM. 6	IM. 7	IM. 8	AV.	SD.
Zr	180	165	160	200	245	165	230	195	193	32
V	140	125	110	170	100	125	85	75	116	31
Cr	28	25	35	28	27	25	35	40	30	6
Y	22	23	25	20	23	20	27	22	23	2
Sc	<10	<10	<10	<10	<10	<10	<10	<10	<10	—
Sr	85	90	95	100	90	100	150	160	109	29
Ba	100	110	95	100	200	245	400	290	193	113
La	30	35	28	30	30	28	40	38	32	5
Nb	<10	<10	<10	<10	<10	<10	<10	<10	<10	—
Rb	126	144	145	140	144	131	129	123	135	9
Ce	113	98	79	72	60	75	63	75	79	18
Th	25	26	28	26	18	19	22	25	24	4
U	7	6	<5	6	<5	5	5	<5	5	1
Cu	20	20	20	10	15	10	15	10	15	5
Ni	14	12	15	17	10	9	20	12	14	4
Co	<10	<10	<10	<10	<10	<10	<10	<10	<10	—
Pb	14	21	27	17	20	20	18	19	20	4
Mo	2	1	1	2	1	1	5	1	2	1
Sn	<10	<10	<10	<10	<10	<10	<10	<10	<10	—
Ag	1.5	<1	<1	<1	<1	<1	<1	<1	<1	—
Bi	<10	<10	<10	<10	<10	<10	<10	<10	<10	—
Cd	<10	<10	<10	<10	<10	<10	<10	<10	<10	—
Zn	<10	20	26	18	32	11	11	10	17	8
W	<10	<10	<10	<10	<10	<10	<10	<10	<10	—
As	<30	<30	<30	<30	<30	<30	<30	<30	<30	—
Sb	<10	<10	<10	<10	<10	<10	<10	<10	<10	—
Rb/Sr	1.48	1.60	1.53	1.40	1.60	1.31	0.86	0.77	1.32	0.33
K/Rb	274	231	226	249	231	254	258	258	248	17

granite belongs to the volcanic arc granite derived from subduction of oceanic crust. This suggestion is also supported by the multicationic parameters for the tectonomagmatic divisions (Batchelor and Bowden, 1985) showing the studied granite compositions are plotted on the destructive plate margin granite.

Rare earth elements (REE) were determined on four representative samples and the analytical results are presented in Table 3. The REE abundance data for these samples have been normalised to the average chondritic contents (Frey et al, 1968), and plotted on a logarithmic scale against atomic number (Fig. 5).

The Imog granite shows light REE enrichement and heavy REE depletion with $(Ce/Yb)N$ ratios of $7.77 \sim 12.55$ (the average ratio being 10.21 ± 2.09). All the REE patterns in the granite have moderate negative Eu anomalies with $Eu/Eu^* = 0.62 \sim 0.77$ (a mean ratio of 0.69). The gradually increasing negative Eu anomaly size is consistent with increased REE fractionation with differentiation. The relatively low Sr content (109 ± 29ppm) and mild negative Eu anomaly are due largely to feldspar fractionations as plagioclase has high phenocryst-matrix partition coefficients for Sr and Eu^{2+}, and high K/Rb ratios (Arth 1976).
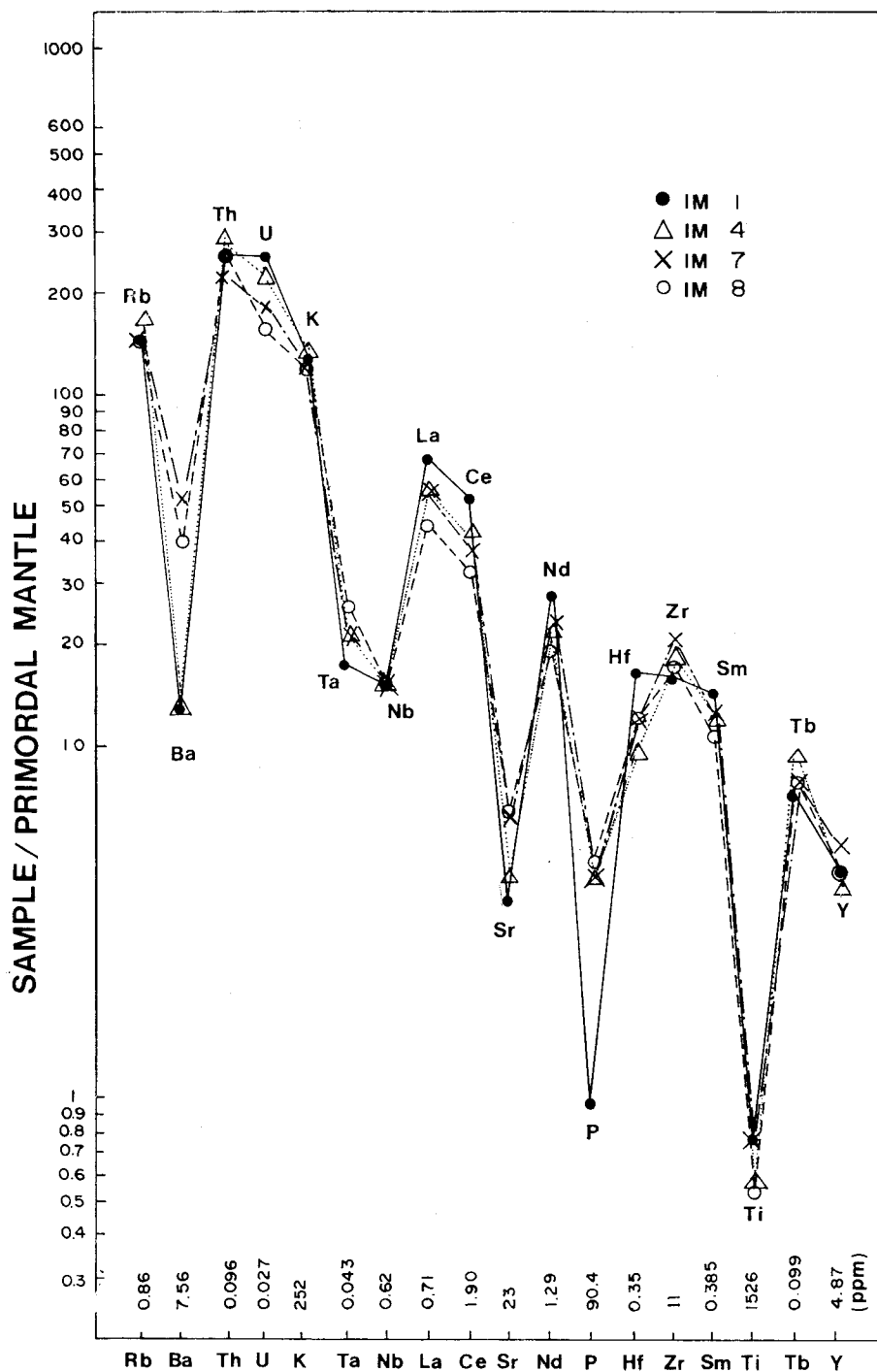
Fig. 4 Abundances of incompatible trace elements in the Imog granite normalised to primordial mantle composition (Wood, 1979).

Table 3 Rare Earth Elements analyses (in ppm) of the Imog granite. The REE contents in the chondrite are after Frey et al (1968). CHON: Chondrite

	IM.1	IM.4	IM.7	IM.8	AV.	SD.	CHON.
La	48.63	39.58	39.41	32.10	39.93	6.77	0.328
Ce	101.76	78.40	74.58	63.71	79.61	16.02	0.865
Nd	36.54	28.44	29.39	25.32	29.92	4.74	0.630
Sm	5.67	4.91	4.92	4.28	4.95	0.57	0.203
Eu	1.26	1.08	1.11	0.91	1.09	0.14	0.077
Gd	4.08	4.42	5.83	4.88	4.80	0.76	0.276
Tb	0.70	0.97	0.84	0.84	0.84	0.11	0.052
Tm	0.29	0.30	0.30	0.31	0.30	0.01	0.034
Yb	1.74	1.87	1.97	2.03	1.90	0.13	0.220
Lu	0.28	0.26	0.28	0.30	0.28	0.03	0.034
ΣREE	200.95	160.23	158.63	134.68	163.62	27.49	2.719
Hf	5.94	3.43	4.47	4.44	4.07	1.89	
Ta	0.76	0.92	0.93	1.15	0.94	0.16	
(Ce/Yb)N	12.55	11.18	9.33	7.77	10.21	2.09	
(La/Yb)N	18.50	14.71	13.33	10.11	14.16	3.48	
(Ce/Yb)	58.48	41.93	37.86	31.38	42.41	11.56	
(La/Yb)	27.95	21.17	20.01	15.81	21.24	5.03	
Eu/Eu*	0.77	0.74	0.64	0.62	0.69	0.07	
ΣCe	193.86	152.41	149.41	126.32	155.50	28.10	
ΣY	7.09	7.82	9.22	8.36	8.12	0.90	

Eu* : Eu value derived by interpolation between Sm and Gd
N   : Chondrite normalised value
ΣCe: Sum of Light REE (LREE): La to Eu
ΣY : Sum of Heavy REE (HREE):Gd to Lu

K/Ar ISOTOPIC AGE

The radiometric age determinations on the Imog granite have been previously revealed as 94Ma (Kim, 1971), 193Ma (Kim and Kim, 1978) and $92\pm1-93\pm1$ (Yun, 1983) by K-Ar dating on biotites.

Pure biotite mineral concentrates are obtained from sample IM8 (Fig. 1b) using conventional magnetic separation techniques(Hutchison, 1974). Potassium determinations were made by flame photometry (IL 551 AA-AE spectrophotometry). Argon was extracted and measured by isotope dilution on a Nuclide 6''-60°-SGA mass spectrometer. The analytical result is provided in Table 4.

Age measured on the Imog granite should be interpreted as the time of cooling to a temperature equal to the argon closure temperature for the biotite (300°$\pm$50°C: Hunziker, 1979).

Table 4 K-Ar age data for the Imog granite. The decay constants proposed by Steiger and Jäger (1977) are used in this work.

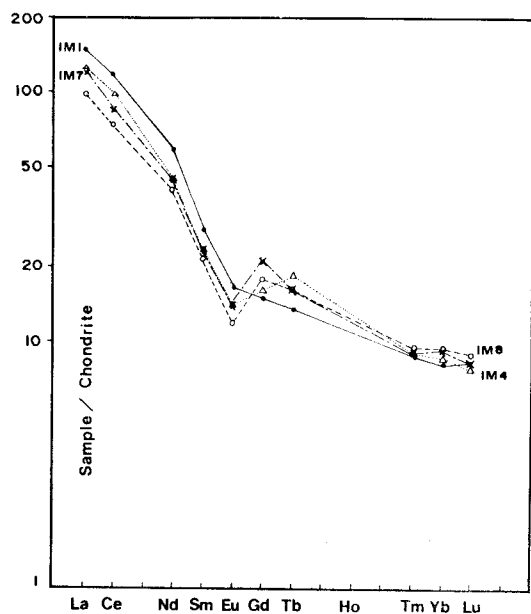| Sample No.	Rock type	Mineral dated	K(%)	^{40}Ar rad (10^{-9} mol/g)	^{40}Ar rad	Age(Ma)
IM.8	Quartz Monzonite	Biotite	7.15	1.551	96.4	96.7$\pm$2.0

Fig. 5 Chondrite-normalised REE abundances in the Imog granite.

DISCUSSION AND CONCLUSIONS

The distribution of plutons and ore deposits around the Hambaeg basin (Fig. la) is generally shown with E-W direction, which is roughly parallel to the synclinal axis of the basin. This implies that tectonic weaknesses such as deep faults and fractures might be existed in the basement with E-W main and N-S subsidiary directions prior to the granitic intrusions. The granitoids around the Hambaeg basin may be intruded along the tectonic intersections of the E-W and N-S lines.

Discussion on the origin of granite resolves around two constrasting hypotheses: fractional crystallization of a more basic parent magma and partial melting of older crustal material. The Imog granite has enriched in Al_2O_3, Na_2O, Rb, Th, U, K, La, Ce, Nd, Hf, Zr, Sm and Tb relative to the Fe_2O_3/FeO, Ba, Ta, Nb, Sr, P, Ti and Y. The major element variation displays generally a cluster trend, but some of trace element such as Rb/Sr-Rb, Ba-Rb, Ba-Sr,

Rb-Sr, Rb-Zr and Ni-Mo shows a continuous trend typical of fractional crystallization. The chondrite normalised rare earth element patterns show mild negative Eu anomalies (Eu/Eu*= 0. 69). The negative anomaly, and low Ba and Sr could arise if plagioclase was one of the early fractionated mineral phases during differentiation. The composition of the granite lies near the ternary minimum of the low-temperature trough in the water-saturated system Q-Or-Ab-An-H_2O (Tuttle and Bowen, 1958). In general, the Imog granite belongs to the magnetite-series based on the magnetic subsceptibility but the ilmenite-series values are seen in some places, especially in the marginal part of the pluton. The ilmenite-series values could be resulted from local reduction due to admixing of the roof and wall carbonaceous and slate xenoliths in the parental magma. In the near-surface brittle environment, the magma moves along fractures and may stop blocks overlying or adjacent country rocks which fall into the magma to form angular country rock xenoliths. These may in time become rounded, further reduced in size, and recrystallized. Incorporation of such xenoliths adds volume to the magma and changes its composition as a result of assimilation (epizonal pluton).

The primary magma of the Imog granite, which is classified as volcanic arc granite-destructive plate margin granite based on tectonic intrusive settings (Pearce et al, 1984, and Batchelor and Bowden, 1985), derived from the subduction of oceanic crust at the destructive plate margin to be squeezed upward through the crust along zones of weakness.

The parental granitic magma of the Imog granite adsorbed meteoric water from the country rocks and then boiled off. The ore mineralization (Fe-Pb-Zn) associated with the granite may be explained as having formed by fractional crystallization, leading to continuous enrichment

of the metallic elements in the melt. During progressive volatile-pressure relief, the metallic elements will eventually fractionate into the escaping fluid phase, thus establishing a basis for the mineralizations.

Radiometric age determination on the Imog granite reveals as 96.7 ± 2.0 Ma by K-Ar dating on biotite, which is the time passed after argon closure temperature of $300 \pm 50°C$ of biotite.

The observations and arguments presented for the Imog granite lead to the following general conclusions:

1) The granite is a calc-alkaline subsolvus monzogranite. It is generally a medium grained pale pinkish feldspar biotite granite, which consists of quartz, microcline-microperthite, oligoclase, biotite, hornblende, apatite, zircon, tourmaline and opaque minerals;

2) The granite has enriched in LIL elements relative to the HFS elements, and show light REE enrichment and heavy REE depletion with $(Ce/Yb)N$ ratios of $7.77 \sim 12.55$. All the REE patterns show Eu negative anomalies $(Eu/Eu^* = 0.62 \sim 0.77)$, which mainly due to feldspar fractionation;

3) The granite shows characteristics of "I-type" granite by mineralogical and chemical compositions. According to the magnetic subsceptibility measurements, the granite belongs to the "magnetite-series" but some "ilmenite-series" values are found as the result of admixing of the carbonaceous (and slate) xenoliths in the parental magma;

4) Age determination on the granite reveals as 96.7 ± 2.0 Ma by K-Ar dating on biotite. The Cretaceous granitoids around the Hambaeg basin may be intruded along the tectonic intersections of the E-W and N-S lines such as deep faults and fractures.

REFERENCES

Arth, J.G. (1976) Behaviour of trace elements during magmatic processes, a summary of theoretical models and their applications. J. of Research of the U.S. Geological Survey. v. 4, p. 41-47.

Batchelor, R.A., and Bowden, P. (1985) Petrogenetic interpretation of granitoid rock series using multicationic parameters. Chemical Geology, v. 48, p. 43-55.

Brown, G.C. (1979) The changing pattern of batholith emplacement during earth history. In: Atherton, M.P. and Tarney, J. (ed.), Origin of granite batholiths, geochemical evidences. Shiva Publ. Ltd., p. 106-115.

Frey, F.A., Haskin, M., Poeta, J. and Haskin, L. (1968) Rare earth abundances in basic rocks. J. of Geophy. Research, v. 73, p. 6085-6098.

Gordon, C.E., Randle, K., Goles, G.G., Corliss, J.B., Beeston, M.H. and Oxley, S.S. (1968) Instrumental activation analysis of standard rocks with high resolution gamma-ray detectors. Geochim. Cosmochim. Acta., v. 32, p. 369-396.

Hine, R., Williams, S.W., Chappell, B.W., and White, A.J.R. (1978) Contrasts between I-and S-type granitoids of the Kosciusko batholith. J. Geol. Soc. Australia, v. 25, p. 219-234.

Hong, Y.K. (1983) Petrology and geochemistry of Jurassic and Cretaceous granties, South Korea. Unpubl. Ph.D. thesis, Univ. of London, 365pp.

Hunziker, J.C. (1979) Potassium Argon dating. In: Lectures in Isotope geology, Springer-Verlag, p. 52-76.

Hutchison, C.S. (1974) Laboratory handbook of petrographic techniques. John Wiley & Sons, Inc. 527pp.

Ishihara, S. (1979) Lateral variation of magnetic

susceptibility of the Japanese granitoids. J. Geol. Soc. Japan, v. 85, p. 509-523.

Ishihara, S., and Ulriksen, C.E. (1980) The magnetite-series and ilmenite-series granitoids in Chile. Mining Geol., v. 30, p. 183-190.

Kim, H.J. (1986) Geochemical characteristics of Imog granite and relation of mineralization. Unpubl. MSc thesis, Kyungpook Nat. Univ., 40pp.

Kim, O.J. (1971) Study on the intrusion epochs of younger granites and their bearing to orognies of South Korea. J. of Korean Inst. Mining Geol., v. 4, p. 1-9.

Kim, O.J., and Kim, K.H. (1978) On the genesis of the ore deposits of the Yemi district in the Taebaegsan metallogenic province. J. Natural Sci. Res. Inst., Yonsei Univ., v. 2, p. 71-94.

Lee, D.S. (1966) Geological map of Ogdong sheet (1/50,000). Geological survey of Korea, 36pp.

O'Connor, J.T. (1965) A classification for quartz-rich igneous rocks based on feldspar ratios. U.S. Geol. Surv. Prof. Paper, 525-b, p. 79.

Pearce, J.A., Harris, N.B.W., and Tindle, A.G. (1984) Trace element discrimination diagram for the tectonic interpretation of granitic rocks. J. of Petrol., v. 25, p. 956-983.

Scintrex Instruction manual (1982) Geophysical and geochemical instrumentation and services. Geophysical instrumental & supply company, 27pp.

Seo, J.R. (1985) A study on geology and Ore deposits of the regional mineralization in the Ogdong sheet. KIER report 85-15, p. 75-122.

Steiger, R.H., and Jäger, E. (1977) Subcommission on geochronology: Convention on the use of decay constants in geo-and cosmochronology. Earth planet. Sci. Lett, v. 36, p. 359-362.

Streckeisen, A. (1976) To each plutonic rocks and its proper name. Earth Sci. Rev., v. 12, p. 1-33.

Tuttle, O.F., and Bowen, N.L. (1958) Origin of granite in the light of experimental studies in the studies in the system $NaAlSi_3O_8-KAlSi_3O_8-SiO_2-H_2O$. Geol. Soc. Am. Memoir, 74.

Wood, D.A. (1979) A variably veined suboceanic upper mantlegenetic significance for mid-Ocean ridge basalts from geochemical evidence. Geology, v. 7, p. 499-503.

Wright, J.B. (1969) A simple alkalinity ratio and its application to questions of non-orogenic granite gneiss. Geol. Mag., v. 106, p. 370-384.

Yun, H.S. (1983) K/Ar ages of micas from precambrian and phanerozoic rocks in northeastern part of the Republic of Korea. Schweiz. Mineral. Petrogr. Mitt., v. 63, p. 295-300.

Yun, H.S. (1985) Petrochemical study on the granitic rocks in the Southern Hambaeg basin and its basement area. Unpubl. Ph.D thesis, Yonsei Univ., 147pp.

咸白盆地 南西部에 分布하는 梨木花崗岩의 地化學 및 K-Ar 年代測定

洪　永　國*

要約 : 梨木花崗岩은 칼크-알카라인 subsolvus 몬조花崗岩에 屬하고 中粒質이며, 石英, 長石, 黑雲母 및 角閃石으로 構成되어 있다.

本 花崗岩은 鑛物組成 및 地化學的 特徵으로 보아 "I-type" 및 "magnetite-series"로 分類된다. 梨木花崗岩의 親마그마가 주위 母岩인 朝鮮累層群의 岩石(主로 石灰岩)을 捕獲하여 同化시킴으로 마그마의 化學的 特性이 一部 變한 것으로 思料된다. 梨木花崗岩은 咸白盆地주위의 構造的 弱線帶인 東西 및 南北方向이 交叉하는 斷層面이나 斷裂帶를 따라서 地殼의 淺部까지 貫入하고 있다.

梨木花崗岩의 本源마그마는 海洋地殼의 subduction으로 因한 上部맨틀의 部分熔融에 依하여 形成되었다. 마그마의 分別結晶作用에 있어서는 長石의 分別作用에 依해 化學的 影響을 크게 받은 것으로 나타났다. 本 花崗岩에서 分離한 黑雲母를 對象으로 K-Ar年代測定을 實施한 結果 96.7±2.0Ma로 밝혀졌다.

---

* 韓國動力資源研究所 地化學探査研究室